

---



# PRISM- $\Delta$ : Differential Subspace Steering for Prompt Highlighting in Large Language Models

---

Yuyao Ge<sup>1</sup> Shenghua Liu<sup>1\*</sup> Yiwei Wang<sup>2</sup> Tianyu Liu<sup>3</sup> Baolong Bi<sup>1</sup>  
Lingrui Mei<sup>1</sup> Jiayu Yao<sup>1</sup> Jiafeng Guo<sup>1</sup> Xueqi Cheng<sup>1</sup>

<sup>1</sup>Institute of Computing Technology, Chinese Academy of Sciences

<sup>2</sup>University of California, Merced <sup>3</sup>Peking University

{geyuyao24z, liushenghua}@ict.ac.cn

 <https://github.com/YuyaoGe/PRISM-DELTA>

## Abstract

Prompt highlighting steers a large language model to prioritize user-specified text spans during generation. A key challenge is extracting steering directions that capture the difference between relevant and irrelevant contexts, rather than shared structural patterns common to both. We propose PRISM- $\Delta$  (**P**rojection-based **R**elevance-**I**nformed **S**teering **M**ethod), which decomposes the difference between positive and negative cross-covariance matrices to maximize discriminative energy while eliminating shared directions. Each attention head receives a continuous softplus importance weight, letting weak-but-useful heads contribute at reduced strength. The framework extends naturally to Value representations, capturing content-channel signal that Key-only methods leave unused. Across four benchmarks and five models, PRISM- $\Delta$  matches or exceeds the best existing method on 19 of 20 configurations, with relative gains up to +10.6%, while halving the fluency cost of steering. PRISM- $\Delta$  also scales to long-context retrieval, outperforming the best existing method by up to +4.8% relative gain. PRISM- $\Delta$  is compatible with FlashAttention and adds negligible memory overhead.

## 1 Introduction

Large language models frequently need to prioritize specific parts of their input. When presented with conflicting information, the model should attend to newly provided facts over its parametric memory. In long-context retrieval, the answer may reside in the middle of thirty passages, where models notoriously underperform [Liu et al., 2024]. This problem is known as *prompt highlighting* [Li et al., 2026]: given a prompt and a marked subset of tokens, the goal is to amplify the model’s attention to those tokens so that generation becomes more accurate and faithful to user intent.

Several prompt highlighting methods have been proposed, including post-hoc attention score manipulation [Zhang et al., 2023], logit-level anchoring [Tian and Zhang, 2024], and pre-attention Key vector editing via spectral decomposition [Li et al., 2026]. However, all of them operate solely on the *routing channel*—Key representations that control where the model looks. Transformer attention output also depends on a *content channel*—Value representations that determine what information is transmitted. Even when routing successfully directs the model to attend to highlighted tokens, the information those tokens convey through their Value representations remains unenhanced.

We investigate whether the Value channel carries useful signal by extracting Key and Value representations under contrastive conditions. Value shifts are comparable in magnitude to Key across all five

---

\*Corresponding author.

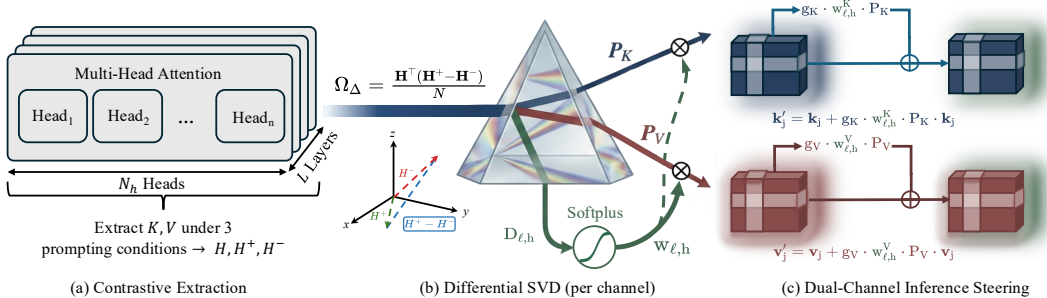


Figure 1: Overview of PRISM- $\Delta$ . SVD decomposes  $\Omega_\Delta$  into per-head projections ( $P_K$ ,  $P_V$ ) and importance weights ( $w_{\ell,h}$ ), steering both Key and Value channels at inference.

tested models, with roughly half of all heads showing significant Value-channel signal. Key-only methods thus leave substantial signal unused.

We propose PRISM- $\Delta$  (**P**rojection-based **R**elevance-Informed **S**teering **M**ethod), which steers both channels through discriminative subspace learning and adaptive head weighting (Figure 1). Our contributions are:

- We introduce *differential cross-covariance decomposition* to extract maximally discriminative directions from contrastive data. Each head’s signal strength is mapped to a continuous softplus weight, enabling adaptive steering that suppresses noisy heads while preserving weak-but-useful ones.
- We extend this framework to *jointly steer Key and Value channels*. The Value channel reduces the fluency degradation caused by steering and improves generation consistency.

PRISM- $\Delta$  consistently outperforms the best existing method on three short-context benchmarks across five models, with relative gains up to +10.6%, and further scales to long-context retrieval with up to +4.8% gain on 30-passage inputs.

## 2 Related work

**Prompt highlighting.** PASTA [Zhang et al., 2023] modifies attention scores post-hoc but is incompatible with FlashAttention [Dao et al., 2022]. SPA [Tian and Zhang, 2024] anchors at the logit level but requires multiple forward passes. SEKA [Li et al., 2026] edits Key vectors via spectral decomposition with near-zero overhead. All three operate exclusively on the routing channel, leaving the content channel unused. PRISM- $\Delta$  differs by jointly steering Key and Value channels with per-head continuous weighting, capturing both routing and content gains. Prefix-Tuning [Li and Liang, 2021] also operates in Key/Value space by prepending learned soft tokens, but requires gradient-based training and modifies the context length; PRISM- $\Delta$  is gradient-free and edits existing token representations in place.

**Activation editing and head specialization.** SEA [Qiu et al., 2024], Representation Engineering [Zou et al., 2023], Inference-Time Intervention [Li et al., 2023], Activation Addition [Turner et al., 2024], instruction-following steering [Stolfo et al., 2024], and CARVE [Ge et al., 2025] modify residual stream or attention activations via contrastive signals but do not distinguish Key and Value roles. Subramani et al. [2022] extract latent steering vectors from pretrained models. In knowledge editing, ROME [Meng et al., 2022], AlphaEdit [Fang et al., 2025], and Hernandez et al. [2023] target factual associations through activation or parameter updates. Clark et al. [2019], Voita et al. [2019], Michel et al. [2019], Elhage et al. [2021], and Olsson et al. [2022] demonstrate that attention heads exhibit functional specialization, while Wu et al. [2025] identify retrieval heads critical for long-context factuality. Per-head importance weighting, rather than uniform steering, is therefore better grounded. PRISM- $\Delta$  uses differential SVD to extract per-head discriminative directions and softplus to assign continuous importance weights; a detailed comparison appears in Table 7 (Appendix B).

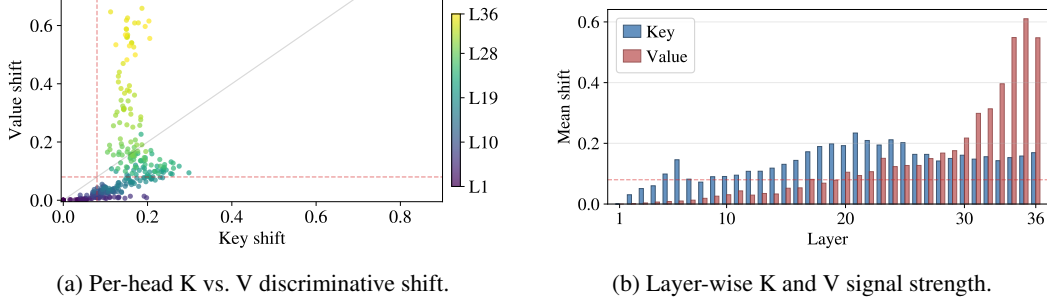


Figure 2: Dual-channel discriminative signals in QWEN3-4B-Base (288 heads). **(a)** Each point is one attention head; Key and Value shifts are weakly correlated ( $r=0.342$ ), confirming that the two channels carry complementary information. **(b)** Key signal peaks in middle layers (L13–24), while Value signal peaks in late layers (L25–36), suggesting functional specialization across depth.

### 3 Method

#### 3.1 Dual-channel view of attention

In standard multi-head attention, given input hidden states  $\mathbf{x}_i$ , each head  $(\ell, h)$  computes:

$$\mathbf{q}_i = W_Q^{(\ell, h)} \mathbf{x}_i, \quad \mathbf{k}_j = W_K^{(\ell, h)} \mathbf{x}_j, \quad \mathbf{v}_j = W_V^{(\ell, h)} \mathbf{x}_j \quad (1)$$

We drop the  $(\ell, h)$  superscripts in subsequent equations for readability.

$$\text{output}_i = \sum_j \underbrace{\text{softmax}\left(\frac{\mathbf{q}_i^\top \mathbf{k}_j}{\sqrt{d}}\right)}_{\alpha_{ij}: \text{routing}} \cdot \underbrace{\mathbf{v}_j}_{\text{content}} \quad (2)$$

**Problem definition.** Given a prompt  $\mathbf{x} = (x_1, \dots, x_T)$  and a set of highlighted tokens  $\mathcal{S} \subset \{1, \dots, T\}$ , the goal is to amplify the influence of tokens  $j \in \mathcal{S}$  in the attention output.

**Dual-channel decomposition.** The attention output is jointly determined by two functionally distinct channels: the *routing channel* ( $\mathbf{K} \rightarrow \alpha$ : determines *where* to look) and the *content channel* ( $\mathbf{V}$ : determines *what* information is transmitted). If we simultaneously perturb both channels for highlighted tokens:

$$\begin{aligned} \text{output}'_i &= \sum_j (\alpha_{ij} + \Delta\alpha_{ij}) \cdot (\mathbf{v}_j + \Delta\mathbf{v}_j) \\ &= \text{output}_i + \underbrace{\sum_j \Delta\alpha_{ij} \cdot \mathbf{v}_j}_{\text{routing gain}} + \underbrace{\sum_j \alpha_{ij} \cdot \Delta\mathbf{v}_j}_{\text{content gain}} + \underbrace{\sum_j \Delta\alpha_{ij} \cdot \Delta\mathbf{v}_j}_{\text{cross gain}} \end{aligned} \quad (3)$$

Existing prompt highlighting methods capture only the routing gain; the content gain and cross gain remain unused. Figure 2 confirms that Key and Value carry complementary signals, with their strength peaking at different network depths.

#### 3.2 Discriminative subspace learning

**Contrastive data and representation extraction.** We construct synthetic QA triplets to identify contrastive directions. For each text context, we extract representations (Key or Value) at the answer token position under three conditions:  $\mathbf{H}$  (neutral, context only),  $\mathbf{H}^+$  (positive, context + relevant question), and  $\mathbf{H}^-$  (negative, context + irrelevant question).

**Differential cross-covariance.** We define the uncentered cross-covariance  $\Omega^+ = \mathbf{H}^\top \mathbf{H}^+ / N$ . Its top singular directions may include *shared* directions that co-vary equally under both conditions. To isolate truly discriminative directions, we decompose the *differential* cross-covariance:

$$\Omega_\Delta = \mathbf{H}^\top (\mathbf{H}^+ - \mathbf{H}^-) / N = \Omega^+ - \Omega^- \quad (4)$$

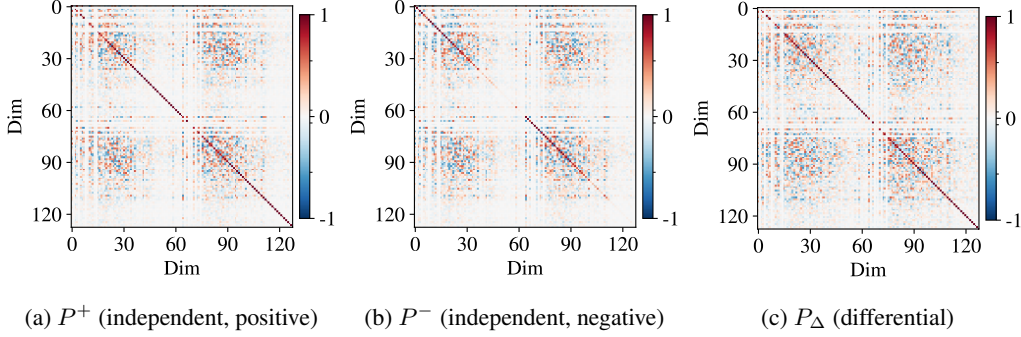


Figure 3: Projection matrix structure for layer 21, head 4 of QWEN3-4B with  $d=128$ . Independent projections  $P^+$  (rank 89) and  $P^-$  (rank 39) exhibit overlapping subspaces ( $\text{tr}(P^+P^-) = 1.31$ ), while the differential projection  $P_\Delta$  (rank 89) directly targets the discriminative subspace.

**Proposition 1** (Discriminative optimality of differential directions). *Let  $\Omega_\Delta = U_\Delta \Sigma_\Delta V_\Delta^\top$  be the SVD of the differential cross-covariance. Then:*

- (a) **Maximum discriminative energy.** *The top- $k$  left singular vectors  $\{u_1, \dots, u_k\}$  solve  $\max_{U \in \mathbb{R}^{d \times k}, U^\top U = I} \|U^\top \Omega_\Delta\|_F^2$ , i.e., they capture the  $k$ -dimensional subspace that maximizes the cross-covariance difference between positive and negative conditions (by the Eckart–Young theorem).*
- (b) **Automatic elimination of shared directions.** *If a direction  $\mathbf{u}_s$  satisfies  $\Omega^+ \mathbf{u}_s = \Omega^- \mathbf{u}_s$ , then  $\Omega_\Delta \mathbf{u}_s = \mathbf{0}$ : shared directions contribute zero to the differential projection, regardless of their energy in  $\Omega^+$ .*

Proposition 1 requires no distributional assumptions; it holds for any finite sample set (proof in Appendix C). Part (a) directly justifies the choice of differential SVD over independent SVD, while part (b) formally explains why shared variance directions are absent from the learned projection.

Figure 3 visualizes the structure of projection matrices for a representative head, showing that independent projections  $P^+$  and  $P^-$  share overlapping column spaces (structural redundancy), while  $P_\Delta$  directly targets the differential subspace.

The top- $k$  left singular vectors form the projection matrix:

$$P = U_\Delta[:, :k] \cdot U_\Delta[:, :k]^\top \quad (5)$$

where  $k$  is chosen such that the cumulative singular value ratio reaches a threshold  $\gamma$ :  $\sum_{i=1}^k \sigma_i / \sum_{i=1}^d \sigma_i \geq \gamma$ .

**Head importance weighting.** Different attention heads vary widely in their sensitivity to prompt highlighting. The SVD process naturally yields a per-head discriminability measure—the norm difference  $D_{\ell,h} = \frac{1}{N} \sum_i \|\mathbf{r}_i^+ - \mathbf{r}_i^-\|_2$  (where  $\mathbf{r}$  denotes the head’s Key or Value representation)—which quantifies how much the head’s output shifts between positive and negative conditions. We map this to a continuous weight via the softplus function:

$$w_{\ell,h} = \text{softplus}(D_{\ell,h} - \delta_{\min}) = \log(1 + \exp(D_{\ell,h} - \delta_{\min})) \quad (6)$$

We choose softplus because it smoothly interpolates between full activation for strong heads ( $D \gg \delta_{\min}$ ) and near-zero contribution for weak ones ( $D \ll \delta_{\min}$ ).

The projection  $P$  and weight  $w$  share the same data signal  $D_{\ell,h}$ : a large  $D$  means the head’s contrastive signal is strong, so its projection is reliable (Proposition 1) and it should receive stronger steering. The two are not independent choices but consequences of a single data-driven measure.

### 3.3 Dual-channel steering

We apply the subspace learning framework (Section 3.2) separately to Key and Value spaces:

$$\text{Key: } \Omega_{\Delta}^K = \mathbf{H}_K^{\top}(\mathbf{H}_K^+ - \mathbf{H}_K^-)/N \xrightarrow{\text{SVD}} P_K, w_K \quad (7)$$

$$\text{Value: } \Omega_{\Delta}^V = \mathbf{H}_V^{\top}(\mathbf{H}_V^+ - \mathbf{H}_V^-)/N \xrightarrow{\text{SVD}} P_V, w_V \quad (8)$$

At inference time, for each highlighted token  $j \in \mathcal{S}$ , both channels are simultaneously edited:

$$\mathbf{k}'_j = \mathbf{k}_j + g_K \cdot w_{\ell,h}^K \cdot P_K \cdot \mathbf{k}_j \quad (9)$$

$$\mathbf{v}'_j = \mathbf{v}_j + g_V \cdot w_{\ell,h}^V \cdot P_V \cdot \mathbf{v}_j \quad (10)$$

where  $g_K, g_V$  are gain scalars controlling the strength of routing and content steering, respectively.

**Geometric interpretation.** Each transformation  $(I + g \cdot w \cdot P) \cdot \mathbf{x}$  amplifies the component of  $\mathbf{x}$  within the learned subspace by a factor of  $(1 + g \cdot w)$  while leaving the orthogonal component unchanged. Unlike uniform amplification, each head’s amplification factor is individually modulated by its discriminability  $w_{\ell,h}$ . This differs from adding a constant bias to the attention logit: Key scaling produces a *query-dependent* boost—the attention shift varies with the semantic content of each query position—whereas logit bias applies a fixed offset regardless of query.

**Instantiations.** PRISM- $\Delta$  admits two variants:

- PRISM- $\Delta$  ( $g_V = 0$ ): steers only the routing channel, with overhead identical to existing Key-editing methods.
- PRISM- $\Delta V$  ( $g_K > 0, g_V > 0$ ): steers both channels, capturing all three gain terms in Eq. 3.

PRISM- $\Delta$  is a special case of PRISM- $\Delta V$  at  $g_V = 0$ ; both share the projection learning framework. The complete pipeline is given in Algorithm 1 (Appendix D).

## 4 Experimental setup

**Benchmarks.** We evaluate on three prompt highlighting benchmarks: **BiasBios** [De-Arteaga et al., 2019] (occupation prediction from highlighted biographies; metrics: Accuracy, Fluency, Consistency), **CounterFact** [Meng et al., 2022] (knowledge conflict resolution; metrics: Efficacy, Paraphrase), and **Pronoun Change** [Li et al., 2026] (rewriting gendered pronouns to gender-neutral forms according to highlighted instructions; metrics: P. Score measures whether the target pronoun was changed, All-changed P. Score requires all pronouns to be changed). Formal metric definitions are in Appendix E; hyperparameters are tuned on held-out validation sets.

**Models.** We evaluate across two architecture families and three scales: QWEN3-4B/8B/14B-Base [Yang et al., 2025] and GEMMA3-4B/12B-PT [Gemma Team, 2025].

**Baselines.** We compare against five baselines: **Original** (no steering), **\*\* -marked** (surrounding highlighted text with asterisks), **PASTA** [Zhang et al., 2023], **SPA** [Tian and Zhang, 2024], and **SEKA** [Li et al., 2026]. A comparison with AdaSEKA, a higher-cost multi-expert variant, is provided in Appendix F.

**PRISM- $\Delta$  configurations.** PRISM- $\Delta$  uses Key-only steering ( $g_V = 0$ ). PRISM- $\Delta V$  steers both Key and Value ( $g_V > 0$ ). Projections are constructed offline from 100 synthetic contrastive QA pairs. Hyperparameters are listed in Appendix G. All experiments use greedy decoding on single NVIDIA H20 GPUs. Full setup details are in Appendix H.

## 5 Results

### 5.1 Main results

Table 1 presents results across all three benchmarks and five models. On BiasBios, PRISM- $\Delta$  achieves the best accuracy on Qwen3 models with relative gains up to +1.6%; on CounterFact, it ties SEKA at

Table 1: Main results across three benchmarks (%). **Bold**: best; underline: second best.

| Model                 | Metric      | Baselines |              |              |              | Ours         |                 |                   |
|-----------------------|-------------|-----------|--------------|--------------|--------------|--------------|-----------------|-------------------|
|                       |             | Original  | **-marked    | PASTA        | SPA          | SEKA         | PRISM- $\Delta$ | PRISM- $\Delta$ V |
| <b>BiasBios</b>       |             |           |              |              |              |              |                 |                   |
| QWEN3-4B              | Accuracy    | 79.80     | 82.94        | 89.58        | 68.00        | <u>90.92</u> | <b>92.38</b>    | 92.36             |
| QWEN3-8B              |             | 76.22     | 80.60        | 86.32        | 37.02        | <u>88.74</u> | <b>89.62</b>    | 89.12             |
| QWEN3-14B             |             | 85.10     | <u>90.94</u> | 88.46        | 57.86        | 90.28        | <b>91.68</b>    | 91.20             |
| GEMMA3-4B             |             | 89.90     | 91.00        | 82.58        | 48.02        | <u>92.42</u> | <b>92.90</b>    | 91.64             |
| GEMMA3-12B            |             | 91.32     | 92.90        | <b>94.72</b> | 46.88        | <u>93.04</u> | 92.22           | 91.94             |
| <b>CounterFact</b>    |             |           |              |              |              |              |                 |                   |
| QWEN3-4B              | Efficacy    | 45.00     | 57.70        | 97.16        | 65.24        | <u>99.02</u> | <b>99.14</b>    | 98.08             |
|                       | Paraphrase  | 45.64     | 52.12        | 96.03        | 57.71        | <b>98.61</b> | <u>98.52</u>    | 96.51             |
| QWEN3-8B              | Efficacy    | 39.04     | 56.24        | 92.70        | 69.26        | <u>99.08</u> | <b>99.24</b>    | 98.46             |
|                       | Paraphrase  | 39.59     | 49.80        | 91.68        | 58.76        | <u>98.96</u> | <b>99.10</b>    | 98.04             |
| QWEN3-14B             | Efficacy    | 37.56     | 45.52        | 76.84        | 84.22        | 98.92        | <b>99.00</b>    | <u>98.98</u>      |
|                       | Paraphrase  | 36.12     | 40.12        | 66.33        | 76.11        | <b>99.02</b> | <u>98.82</u>    | 98.72             |
| GEMMA3-4B             | Efficacy    | 55.04     | 57.56        | 78.36        | 93.90        | 98.04        | <b>98.10</b>    | 97.68             |
|                       | Paraphrase  | 47.77     | 45.82        | 59.53        | 91.92        | <b>98.83</b> | 96.24           | <u>96.01</u>      |
| GEMMA3-12B            | Efficacy    | 45.34     | 48.72        | 68.30        | 93.76        | <b>98.86</b> | <b>98.86</b>    | 93.40             |
|                       | Paraphrase  | 37.21     | 36.69        | 71.72        | 91.24        | <u>99.27</u> | <b>99.30</b>    | 91.86             |
| <b>Pronoun Change</b> |             |           |              |              |              |              |                 |                   |
| QWEN3-4B              | P. Score    | 93.14     | 95.76        | <u>95.82</u> | 80.27        | 95.18        | <b>96.18</b>    | 96.06             |
|                       | All-changed | 90.52     | 93.88        | <u>94.64</u> | 78.19        | 93.26        | <b>94.60</b>    | 94.52             |
| QWEN3-8B              | P. Score    | 98.00     | 98.10        | <u>98.86</u> | 72.61        | 98.56        | 99.40           | <b>99.48</b>      |
|                       | All-changed | 97.84     | 97.84        | <u>98.72</u> | 74.95        | 98.26        | 99.30           | <b>99.34</b>      |
| QWEN3-14B             | P. Score    | 98.42     | <u>98.86</u> | 90.98        | 91.60        | 98.66        | <b>99.66</b>    | <b>99.66</b>      |
|                       | All-changed | 98.22     | <u>98.68</u> | 90.94        | 92.20        | 98.54        | <b>99.56</b>    | <b>99.56</b>      |
| GEMMA3-4B             | P. Score    | 41.34     | 38.86        | 67.39        | <u>76.05</u> | 81.53        | 89.08           | <b>90.16</b>      |
|                       | All-changed | 35.25     | 32.45        | 66.43        | <u>74.45</u> | 81.11        | 90.58           | <b>91.68</b>      |
| GEMMA3-12B            | P. Score    | 93.92     | 95.78        | 68.47        | 86.41        | <u>97.70</u> | <b>97.94</b>    | 94.54             |
|                       | All-changed | 94.96     | 96.42        | 68.01        | 84.99        | <u>97.24</u> | <b>97.46</b>    | 94.42             |

Table 2: Ablation study on BiasBios (Top-1 Accuracy %). Shaded rows: factorial controls isolating each component.  $\Delta$ : relative improvement (%) over Vanilla.

| Configuration                            | Projection              | Weighting            | Channels | QWEN3-4B     |              | QWEN3-8B     |              |
|--|-------------------------|----------------------|----------|--------------|--------------|--------------|--------------|
|  |                         |                      |          | Acc          | $\Delta$     | Acc          | $\Delta$     |
| PRISM- $\Delta$ V                        | Diff. $\Omega_{\Delta}$ | Softplus             | K+V      | 92.36        | +15.7        | 89.12        | +16.9        |
| PRISM- $\Delta$ (-V)                     | Diff. $\Omega_{\Delta}$ | Softplus             | K only   | <b>92.38</b> | <b>+15.8</b> | <b>89.62</b> | <b>+17.6</b> |
| PRISM- $\Delta$ -V (-K)                  | Diff. $\Omega_{\Delta}$ | Softplus             | V only   | 82.44        | +3.3         | 79.16        | +3.9         |
| -Differential                            | Independent             | Softplus             | K only   | 91.52        | +14.7        | 88.90        | +16.6        |
| -Softplus                                | Differential            | Uniform $w=1$        | K only   | 91.42        | +14.6        | 88.22        | +15.7        |
| -Both                                    | Independent             | Uniform $w=1$        | K only   | 91.44        | +14.6        | 88.50        | +16.1        |
| <i>Baselines</i>                         |                         |                      |          |              |              |              |              |
| SEKA [Li et al., 2026] ( $\delta=0.08$ ) | Dual indep.             | Binary               | K only   | 89.56        | +12.2        | 85.52        | +12.2        |
| SEKA [Li et al., 2026] (default)         | Dual indep.             | Binary $\delta=0.12$ | K only   | 90.92        | +13.9        | 88.26        | +15.8        |
| Vanilla                                  | —                       | —                    | —        | 79.80        | —            | 76.22        | —            |

98.86% on GEMMA3-12B and reaches 99.24% on QWEN3-8B; on Pronoun Change, our methods outperform SEKA on all 5 models with relative gains up to +10.6%. Including Lost-in-the-Middle (Table 3), our methods match or exceed the best existing method on 19 out of 20 model  $\times$  benchmark configurations. The weaker performance on GEMMA3-12B (BiasBios) correlates with higher Key signal magnitude (Appendix I).

**Statistical reliability.** Statistical reliability is high: across five projection subsets, standard deviation is 0.05–0.15%, and PRISM- $\Delta$  matches or exceeds SEKA on 14 out of 15 model  $\times$  benchmark cells ( $p < 0.001$ ). Detailed variance analysis is in Appendix J and sign test derivations in Appendix K.

**PRISM- $\Delta$  vs. PRISM- $\Delta$ V.** On Pronoun Change, PRISM- $\Delta$ V surpasses PRISM- $\Delta$  on GEMMA3-4B by +1.08%, demonstrating that dual-channel steering can yield accuracy gains. On BiasBios the two are within 0.1%. We recommend PRISM- $\Delta$  as the default and PRISM- $\Delta$ V when generation quality is prioritized; see Section 6.2 for a detailed decomposition and Appendix L for  $g_V$  sensitivity.

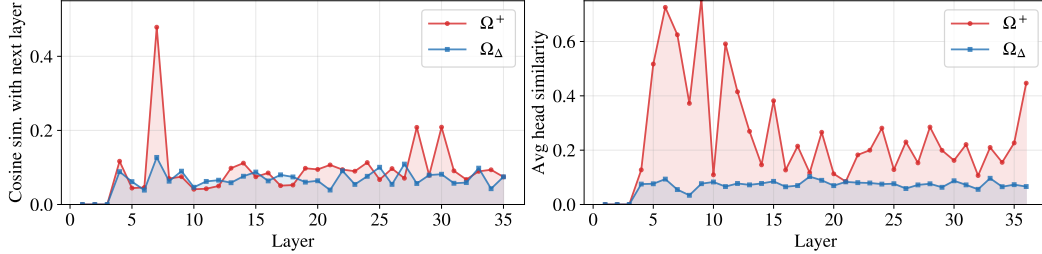


Figure 4: Direction consistency analysis.  $\Omega^+$  directions show high cross-head similarity (dominated by shared structural directions), while  $\Omega_\Delta$  directions are nearly independent (close to random baseline), confirming that differential projection extracts head-specific discriminative directions.

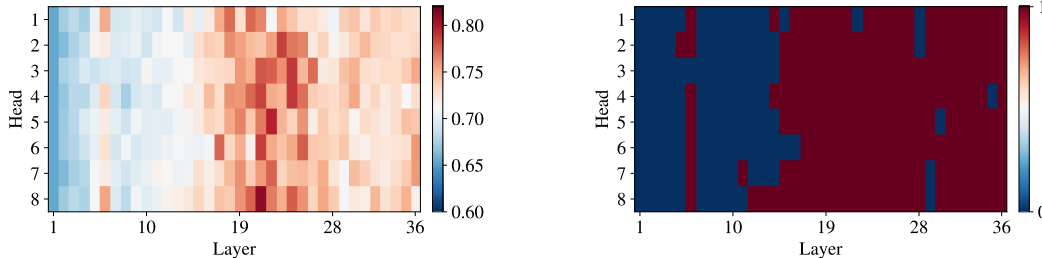


Figure 5: Head weight heatmaps (36 layers  $\times$  8 heads). **Left:** PRISM- $\Delta$  softplus weights show continuous gradation across 288 heads (range [0.654, 0.808]). **Right:** SEKA hard threshold ( $\delta=0.12$ ) creates a binary partition, shutting off 108 heads entirely—including 90% of early-layer heads.

## 5.2 Ablation study

Table 2 uses a  $2 \times 2$  factorial design. Removing softplus costs 0.96% and removing differential projection costs 0.86% on QWEN3-4B. The interaction is strongly super-additive: from the —Both baseline, differential projection alone yields  $-0.02\%$  while softplus alone yields  $+0.08\%$ , yet their combination yields  $+0.94\%$ . This coupling is expected—differential decomposition admits more heads by lowering the effective threshold, and softplus is needed to down-weight the noisy ones among them. At matched  $\delta_{\min}=0.08$ , PRISM- $\Delta$  achieves its best result while SEKA drops by 1.36%, because softplus smoothly down-weights noisy heads rather than giving all activated heads equal weight. PRISM- $\Delta$ -V alone reaches 82.44%, confirming that the Value channel carries independently useful discriminative signal. A CounterFact ablation (Appendix M), data quantity ablation (Appendix N), and projection rank analysis (Appendix O) corroborate these findings.

## 5.3 Lost-in-the-Middle

Table 3 evaluates on the lost-in-the-middle benchmark [Liu et al., 2024] (setup in Appendix H), where steering is applied selectively to the middle region of 30-passage contexts. Our methods match or exceed SEKA on all 5 models, with relative gains up to  $+4.8\%$  on QWEN3-8B, confirming that PRISM- $\Delta$  scales to long-context retrieval.

Table 3: Lost-in-the-Middle: Average Exact Match (%) across 7 gold positions. Steering targets the middle region (passages 4–25). Setup details in Appendix H.

| Model      | Vanilla | SEKA         | PRISM- $\Delta$ | PRISM- $\Delta$ V |
|------------|---------|--------------|-----------------|-------------------|
| QWEN3-4B   | 45.47   | 49.14        | <b>51.43</b>    | 50.57             |
| QWEN3-8B   | 46.69   | 50.29        | <b>52.71</b>    | 51.86             |
| QWEN3-14B  | 57.13   | 60.86        | <b>62.57</b>    | 62.00             |
| GEMMA3-4B  | 44.36   | 47.71        | 49.29           | <b>50.14</b>      |
| GEMMA3-12B | 51.64   | <b>55.57</b> | 54.43           | <b>55.57</b>      |

Table 4: Inference efficiency on QWEN3-8B (batch size 10, avg. 4362 tokens).

| Method            | Avg. Latency (s) | Relative | Peak Mem (GB) | FlashAttn |
|-------------------|------------------|----------|---------------|-----------|
| Original          | 1.180            | 1.0×     | 26.39         | ✓         |
| SEKA              | 1.194 (+0.01)    | 1.0×     | 26.43 (+0.04) | ✓         |
| PRISM- $\Delta$   | 1.481 (+0.30)    | 1.26×    | 26.41 (+0.02) | ✓         |
| PRISM- $\Delta$ V | 1.502 (+0.32)    | 1.26×    | 26.43 (+0.04) | ✓         |

Table 5: Dual-channel decomposition on BiasBios (QWEN3-4B). Best per metric in **bold**. Fluency Cost = Vanilla Fluency – Method Fluency.

| Configuration                    | Top-1 Acc (%) | Fluency ( $\uparrow$ ) | Consistency ( $\uparrow$ ) | Fluency Cost ( $\downarrow$ ) |
|----------------------------------|---------------|------------------------|----------------------------|-------------------------------|
| Vanilla                          | 79.80         | 4.638                  | 0.116                      | 0.000                         |
| SEKA                             | 90.92         | 3.681                  | 0.112                      | 0.957                         |
| PRISM- $\Delta$                  | <b>92.38</b>  | 4.134                  | <b>0.127</b>               | <b>0.504</b>                  |
| PRISM- $\Delta$ -V               | 82.44         | <b>4.666</b>           | 0.121                      | -0.028                        |
| PRISM- $\Delta$ V ( $g_V=0.10$ ) | 92.36         | 4.116                  | 0.125                      | 0.522                         |

## 5.4 Efficiency analysis

As shown in Table 4, SEKA adds negligible overhead (+0.01 s, +0.04 GB) over the original model. PRISM- $\Delta$  adds +0.30 s latency (1.26 $\times$ ) due to the per-head softplus weight computation and weighted projection, with negligible additional memory (+0.02 GB). PRISM- $\Delta$ V adds a further +0.02 s for Value editing. Both variants remain fully compatible with FlashAttention [Dao et al., 2022, Dao, 2023]. For comparison, PASTA adds +1.03 s and +23.12 GB, and SPA adds +5.32 s [Li et al., 2026], placing PRISM- $\Delta$  in between SEKA and these heavier alternatives.

## 6 Analysis

### 6.1 Discriminative subspace quality

We validate the theoretical motivation of differential projection (Proposition 1) through two analyses on QWEN3-4B-Base.

**Direction consistency.** Figure 4 tracks the similarity of top singular directions across layers and heads. **Left:** adjacent-layer similarity measures how much a head’s direction changes from one layer to the next.  $\Omega^+$  directions are highly correlated across layers (0.2–0.4), while  $\Omega_\Delta$  directions shift substantially between layers ( $<0.1$ ), indicating layer-specific discriminative structure. **Right:**

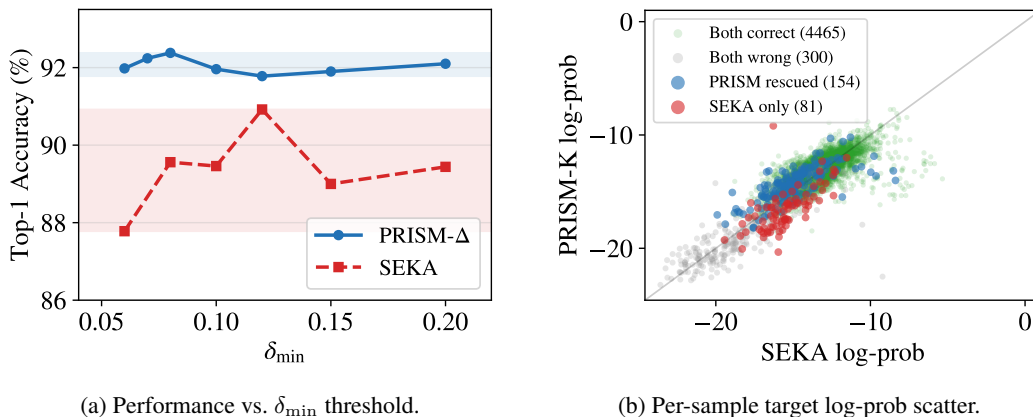


Figure 6: Head selection robustness on BiasBios, QWEN3-4B. (a) PRISM- $\Delta$  maintains stable performance across  $\delta_{\min}$ , while SEKA drops sharply. (b) SEKA (x) vs. PRISM- $\Delta$  (y): PRISM- $\Delta$  rescues 154 samples (blue), loses 81 (red), net +73.

within-layer head similarity measures redundancy among heads in the same layer.  $\Omega^+$  heads converge to similar directions (up to 0.7 in early layers), while  $\Omega_\Delta$  heads remain near-independent throughout all layers. Aggregate statistics are in Table 17 (Appendix P).

**Head weight distribution.** Figure 5 compares softplus weighting with hard thresholding. Hard thresholding shuts off 108 of 288 heads entirely, while softplus assigns them weights of  $\sim 0.69$ , allowing weak-but-useful heads to contribute at reduced strength.

## 6.2 Dual-channel contribution decomposition

Table 5 reveals that the Key channel primarily drives accuracy (+12.58% over Vanilla), while the Value channel preserves generation quality. PRISM- $\Delta$  incurs only 53% of SEKA’s fluency cost. Both PRISM- $\Delta$  and PRISM- $\Delta$ V simultaneously outperform SEKA on all three metrics.

**Layer-wise signal complementarity.** Figure 2b shows that the two channels have complementary depth profiles. Key signal averages 0.175 in middle layers and Value averages 0.307 in late layers, with Value surpassing Key from L28 onward. Key directs attention in middle layers while Value enriches transmitted information in late layers—a functional division rather than redundancy. On Pronoun Change with GEMMA3-4B, PRISM- $\Delta$ V outperforms PRISM- $\Delta$  by 1.08%, confirming that dual-channel steering can surpass Key-only steering on accuracy as well.

## 6.3 Head selection robustness

Figure 6a sweeps  $\delta_{\min}$  from 0.06 to 0.20. SEKA drops by 3.14% from its optimum when  $\delta_{\min}$  is reduced from 0.12 to 0.06: hard thresholding gives all activated heads equal weight  $w=1$ , so including noisy heads degrades performance. PRISM- $\Delta$  fluctuates by only 0.60% across the same range, because softplus automatically assigns lower weights to less discriminative heads. This robustness substantially reduces tuning cost (full sweeps over  $g_K$ ,  $\delta_{\min}$ , and  $\gamma$  are in Appendix Q). Figure 6b plots per-sample target log-probabilities: the majority of samples cluster in the upper-right (both correct) or lower-left (both wrong), while off-diagonal points reveal where the methods diverge. PRISM- $\Delta$  rescues 154 samples that SEKA misclassifies (blue, above diagonal) while losing only 81 (red, below), for a net gain of +73. The 2:1 asymmetry reflects systematic correction of shared-feature confusion, consistent with the shared-direction elimination of Proposition 1(b). Qualitative examples are in Appendix R.

## 7 Conclusion

We presented PRISM- $\Delta$ , which steers both the routing and content channels of Transformer attention for prompt highlighting using differential cross-covariance decomposition and softplus head weighting. Key steering dominates accuracy gains while Value steering reduces fluency degradation. The complementary depth profiles of Key and Value signals suggest a functional division that may be useful for other token-level attention interventions and informs future steering research.

## Limitations

The main practical limitation is that the optimal gain  $g_K$  varies across benchmarks and models, requiring a validation sweep (typically 5–8 values). On Gemma3 models, optimal hyperparameters diverge more from Qwen3 defaults, and GEMMA3-12B on Pronoun Change requires a negative gain—a pattern shared with SEKA [Li et al., 2026], reflecting that the sign of  $g_K$  depends on whether the model’s default tendency aligns with the learned contrastive direction. On near-saturated benchmarks like CounterFact, absolute gains are inherently small for all steering methods. Prompt highlighting gives users control over which input spans the model prioritizes. Misuse risks (e.g., amplifying misleading spans) can be mitigated by restricting highlighting to system-level prompts.

## References

- Kevin Clark, Urvashi Khandelwal, Omer Levy, and Christopher D Manning. What does bert look at? an analysis of bert’s attention. In *Proceedings of the 2019 ACL workshop BlackboxNLP: analyzing and interpreting neural networks for NLP*, pages 276–286, 2019.
- Tri Dao. Flashattention-2: Faster attention with better parallelism and work partitioning. *arXiv preprint arXiv:2307.08691*, 2023.
- Tri Dao, Dan Fu, Stefano Ermon, Atri Rudra, and Christopher Ré. Flashattention: Fast and memory-efficient exact attention with io-awareness. *Advances in neural information processing systems*, 35: 16344–16359, 2022.
- Maria De-Arteaga, Alexey Romanov, Hanna Wallach, Jennifer Chayes, Christian Borgs, Alexandra Chouldechova, Sahin Geyik, Krishnaram Kenthapadi, and Adam Tauman Kalai. Bias in bios: A case study of semantic representation bias in a high-stakes setting. In *proceedings of the Conference on Fairness, Accountability, and Transparency*, pages 120–128, 2019.
- Nelson Elhage, Neel Nanda, Catherine Olsson, Tom Henighan, Nicholas Joseph, Ben Mann, Amanda Askell, Yuntao Bai, Anna Chen, Tom Conerly, et al. A mathematical framework for transformer circuits. *Transformer Circuits Thread*, 1(1):12, 2021.
- Junfeng Fang, Houcheng Jiang, Kun Wang, Yunshan Ma, Jie Shi, Xiang Wang, Xiangnan He, and Tat-Seng Chua. Alphaedit: Null-space constrained model editing for language models. In *The Thirteenth International Conference on Learning Representations*, 2025.
- Yuyao Ge, Shenghua Liu, Yiwei Wang, Lingrui Mei, Baolong Bi, Xuanshan Zhou, Jiayu Yao, Jiafeng Guo, and Xueqi Cheng. Focusing by contrastive attention: Enhancing vlms’ visual reasoning, 2025. URL <https://arxiv.org/abs/2509.06461>.
- Gemma Team. Gemma 3 technical report, 2025. URL <https://arxiv.org/abs/2503.19786>.
- Evan Hernandez, Belinda Z Li, and Jacob Andreas. Inspecting and editing knowledge representations in language models. *arXiv preprint arXiv:2304.00740*, 2023.
- Kenneth Li, Oam Patel, Fernanda Viégas, Hanspeter Pfister, and Martin Wattenberg. Inference-time intervention: Eliciting truthful answers from a language model. *Advances in Neural Information Processing Systems*, 36:41451–41530, 2023.
- Weixian Waylon Li, Yuchen Niu, Yongxin Yang, Keshuang Li, Tiejun Ma, and Shay B Cohen. Spectral attention steering for prompt highlighting. *arXiv preprint arXiv:2603.01281*, 2026.
- Xiang Lisa Li and Percy Liang. Prefix-tuning: Optimizing continuous prompts for generation. In *Proceedings of the 59th Annual Meeting of the Association for Computational Linguistics and the 11th International Joint Conference on Natural Language Processing (Volume 1: Long Papers)*, pages 4582–4597, 2021.
- Nelson F Liu, Kevin Lin, John Hewitt, Ashwin Paranjape, Michele Bevilacqua, Fabio Petroni, and Percy Liang. Lost in the middle: How language models use long contexts. *Transactions of the association for computational linguistics*, 12:157–173, 2024.
- Kevin Meng, David Bau, Alex Andonian, and Yonatan Belinkov. Locating and editing factual associations in gpt. *Advances in neural information processing systems*, 35:17359–17372, 2022.
- Paul Michel, Omer Levy, and Graham Neubig. Are sixteen heads really better than one? *Advances in neural information processing systems*, 32, 2019.
- Catherine Olsson, Nelson Elhage, Neel Nanda, Nicholas Joseph, Nova DasSarma, Tom Henighan, Ben Mann, Amanda Askell, Yuntao Bai, Anna Chen, et al. In-context learning and induction heads. *arXiv preprint arXiv:2209.11895*, 2022.
- Yifu Qiu, Zheng Zhao, Yftah Ziser, Anna Korhonen, Edoardo Maria Ponti, and Shay Cohen. Spectral editing of activations for large language model alignment. *Advances in Neural Information Processing Systems*, 37:56958–56987, 2024.

- Alessandro Stolfo, Vidhisha Balachandran, Safoora Yousefi, Eric Horvitz, and Besmira Nushi. Improving instruction-following in language models through activation steering. *arXiv preprint arXiv:2410.12877*, 2024.
- Nishant Subramani, Nivedita Suresh, and Matthew E Peters. Extracting latent steering vectors from pretrained language models. In *Findings of the Association for Computational Linguistics: ACL 2022*, pages 566–581, 2022.
- Yuan Tian and Tianyi Zhang. Selective prompt anchoring for code generation. *arXiv preprint arXiv:2408.09121*, 2024.
- Alexander Matt Turner, Lisa Thiergart, Gavin Leech, David Udell, Juan J Vazquez, Ulisse Mini, and Monte MacDiarmid. Steering language models with activation engineering, 2024. *URL <https://arxiv.org/abs/2308.10248>*, 2308, 2024.
- Elena Voita, David Talbot, Fedor Moiseev, Rico Sennrich, and Ivan Titov. Analyzing multi-head self-attention: Specialized heads do the heavy lifting, the rest can be pruned. In *Proceedings of the 57th annual meeting of the association for computational linguistics*, pages 5797–5808, 2019.
- Wenhao Wu, Yizhong Wang, Guangxuan Xiao, Hao Peng, and Yao Fu. Retrieval head mechanistically explains long-context factuality. In *13th International Conference on Learning Representations, ICLR 2025*, pages 33762–33775. International Conference on Learning Representations, ICLR, 2025.
- An Yang, Anfeng Li, Baosong Yang, Beichen Zhang, Binyuan Hui, Bo Zheng, Bowen Yu, Chang Gao, Chengen Huang, Chenxu Lv, et al. Qwen3 technical report. *arXiv preprint arXiv:2505.09388*, 2025.
- Qingru Zhang, Chandan Singh, Liyuan Liu, Xiaodong Liu, Bin Yu, Jianfeng Gao, and Tuo Zhao. Tell your model where to attend: Post-hoc attention steering for llms. *arXiv preprint arXiv:2311.02262*, 2023.
- Andy Zou, Long Phan, Sarah Chen, James Campbell, Phillip Guo, Richard Ren, Alexander Pan, Xuwang Yin, Mantas Mazeika, Ann-Kathrin Dombrowski, et al. Representation engineering: A top-down approach to ai transparency. *arXiv preprint arXiv:2310.01405*, 2023.

## A Notation

Table 6: Notation used throughout the paper.

| Symbol                                     | Definition   | Description  |
|--|--|--|
| <i>Model architecture</i>                  |  |  |
| $L$  | Number of layers   | Total Transformer layers in the model                          |
| $n_h$                                      | Number of heads  | Attention heads per layer                                      |
| $d$  | Head dimension   | Dimensionality of each head’s Key/Value space                  |
| $(\ell, h)$                                | Layer-head index   | Identifies a specific attention head                           |
| $\mathbf{x}_j$                             | Token embedding  | Input representation of token $j$                              |
| $W_Q, W_K, W_V$                            | Projection matrices  | Linear projections for Query, Key, Value                       |
| $\mathbf{k}_j, \mathbf{v}_j$               | Key/Value vectors  | Per-token Key and Value representations ( $\in \mathbb{R}^d$ ) |
| $\alpha_{ij}$                              | Attention weight   | Softmax-normalized attention from token $i$ to $j$             |
| <i>Contrastive representations</i>         |  |  |
| $\mathbf{H} \in \mathbb{R}^{N \times d}$   | Neutral representations  | Key (or Value) matrix under context-only condition             |
| $\mathbf{H}^+ \in \mathbb{R}^{N \times d}$ | Positive representations   | Key (or Value) matrix under relevant-question condition        |
| $\mathbf{H}^- \in \mathbb{R}^{N \times d}$ | Negative representations   | Key (or Value) matrix under irrelevant-question condition      |
| $N$  | Number of samples  | Contrastive triplets used for projection construction          |
| <i>Cross-covariance and SVD</i>            |  |  |
| $\Omega^+$                                 | $\mathbf{H}^\top \mathbf{H}^+ / N$                                   | Uncentered cross-covariance (neutral $\times$ positive)        |
| $\Omega^-$                                 | $\mathbf{H}^\top \mathbf{H}^- / N$                                   | Uncentered cross-covariance (neutral $\times$ negative)        |
| $\Omega_\Delta$                            | $\Omega^+ - \Omega^-$  | Differential cross-covariance                                  |
| $U, \Sigma, V$                             | SVD of $\Omega_\Delta$   | Left/right singular vectors and singular values                |
| $k$  | Retained rank  | Number of top singular vectors retained (set by $\gamma$ )     |
| <i>PRISM parameters</i>                    |  |  |
| $P_K, P_V$                                 | $U_{:::k} U_{:::k}^\top$   | Projection matrices for Key and Value channels                 |
| $D_{\ell,h}$                               | $\frac{1}{N} \sum_i \ \mathbf{r}_i^+ - \mathbf{r}_i^-\ _2$           | Per-head discriminability score                                |
| $w_{\ell,h}$                               | $\text{softplus}(D_{\ell,h} - \delta_{\min})$                        | Per-head importance weight                                     |
| $\gamma$                                   | Variance threshold   | Cumulative singular value ratio for rank selection             |
| $\delta_{\min}$                            | Minimum discriminability   | Softplus shift parameter                                       |
| $g_K, g_V$                                 | Gain parameters  | Steering strength for Key and Value channels                   |
| <i>Steering formulas</i>                   |  |  |
| $\mathbf{k}'_j$                            | $\mathbf{k}_j + g_K \cdot w_{\ell,h}^K \cdot P_K \cdot \mathbf{k}_j$ | Steered Key vector for highlighted token $j$                   |
| $\mathbf{v}'_j$                            | $\mathbf{v}_j + g_V \cdot w_{\ell,h}^V \cdot P_V \cdot \mathbf{v}_j$ | Steered Value vector for highlighted token $j$                 |

## B Method comparison

Table 7: Comparison of prompt highlighting methods. AdaSEKA is a multi-expert extension of SEKA with significantly higher overhead; see Appendix F for full comparison.

| Method                             | Steering target       | Projection       | Head selection  | FlashAttn    | Overhead              |
|------------------------------------|-----------------------|------------------|-----------------|--------------|-----------------------|
| PASTA                              | Attn. matrix $\alpha$ | None             | Profiling       | $\times$     | +1.03 s, +23 GB       |
| SPA                                | Logit distribution    | None             | None            | $\checkmark$ | +5.32 s               |
| SEKA                               | Key                   | Indep. SVD       | Hard threshold  | $\checkmark$ | +0.01 s, +0.04 GB     |
| AdaSEKA                            | Key (multi-expert)    | Indep. SVD       | Hard threshold  | $\checkmark$ | +0.27 s, +15.6 GB     |
| <b>PRISM-<math>\Delta</math></b>   | <b>Key</b>            | <b>Diff. SVD</b> | <b>Softplus</b> | $\checkmark$ | <b>+0.30 s, +0 GB</b> |
| <b>PRISM-<math>\Delta V</math></b> | <b>Key + Value</b>    | <b>Diff. SVD</b> | <b>Softplus</b> | $\checkmark$ | <b>+0.32 s, +0 GB</b> |

## C Proof of Proposition 1

*Proof.* **Part (a)** follows directly from the Eckart–Young–Mirsky theorem: for any matrix  $M \in \mathbb{R}^{m \times n}$  with SVD  $M = U \Sigma V^\top$ , the rank- $k$  truncation  $M_k = U[:, : k] \Sigma[:, : k] V[:, : k]^\top$  minimizes

$\|M - M_k\|_F$  over all rank- $k$  matrices. Equivalently,  $U[:, : k]$  maximizes  $\|U[:, : k]^\top M\|_F^2$  over all  $k$ -column orthonormal matrices. Applying this to  $M = \Omega_\Delta$  gives part (a).

**Part (b):** If  $\Omega^+ \mathbf{u}_s = \Omega^- \mathbf{u}_s$ , then  $\Omega_\Delta \mathbf{u}_s = (\Omega^+ - \Omega^-) \mathbf{u}_s = \mathbf{0}$ , so  $\mathbf{u}_s$  lies in the null space of  $\Omega_\Delta$  and receives zero weight in any SVD-based projection.  $\square$

## D Algorithm

Algorithm 1 provides the complete PRISM- $\Delta$  pipeline in pseudocode. The offline stage constructs per-head projection matrices and importance weights from synthetic contrastive data. The online stage applies these projections at inference time via forward hooks, modifying Key and Value representations for highlighted tokens only.

---

### Algorithm 1 PRISM- $\Delta$ : Offline Projection Learning + Online Inference Steering

---

```

1: Input: Model  $\mathcal{M}$  with  $L$  layers,  $n_h$  heads per layer; synthetic QA pairs  $\{(c_i, q_i^+, q_i^-)\}_{i=1}^N$ ;
   hyperparameters  $\gamma, \delta_{\min}, g_K, g_V$ 

2: // — Offline: Projection Learning (per layer  $\ell$ , per head  $h$ ) —
3: for each layer  $\ell = 1, \dots, L$  and head  $h = 1, \dots, n_h$  do
4:   Extract Key representations:  $\mathbf{H}, \mathbf{H}^+, \mathbf{H}^- \in \mathbb{R}^{N \times d}$  under neutral/positive/negative conditions
5:   Compute differential cross-covariance:  $\Omega_\Delta^K = \mathbf{H}^\top (\mathbf{H}^+ - \mathbf{H}^-) / N$ 
6:   SVD:  $\Omega_\Delta^K = U \Sigma V^\top$ ; retain top- $k$  vectors where cumulative energy  $\geq \gamma$ 
7:   Projection matrix:  $P_K = U_{:, :k} U_{:, :k}^\top$ 
8:   Discriminability score:  $D_{\ell, h} = \frac{1}{N} \sum_i \|\mathbf{r}_i^+ - \mathbf{r}_i^-\|_2$ 
9:   Head weight:  $w_{\ell, h}^K = \text{softplus}(D_{\ell, h} - \delta_{\min})$ 
10:  // Repeat for Value channel to obtain  $P_V$  and  $w_{\ell, h}^V$ 
11: end for

12: // — Online: Inference Steering —
13: Input: Prompt tokens with highlighted subset  $\mathcal{S}$ 
14: for each layer  $\ell$ , head  $h$ , token  $j \in \mathcal{S}$  do
15:    $\mathbf{k}'_j = \mathbf{k}_j + g_K \cdot w_{\ell, h}^K \cdot P_K \cdot \mathbf{k}_j$ 
16:    $\mathbf{v}'_j = \mathbf{v}_j + g_V \cdot w_{\ell, h}^V \cdot P_V \cdot \mathbf{v}_j$ 
17: end for
18: Proceed with standard attention:  $\text{softmax}(QK'^\top / \sqrt{d}) \cdot V'$ 

```

---

The offline stage requires  $L \times n_h$  SVD decompositions, each on a  $d \times d$  matrix. For QWEN3-4B with  $d=128$ , this takes approximately 5 minutes on a single GPU. The resulting projection files are stored and reused across all inference runs. The online stage adds a single matrix-vector multiplication per head per highlighted token, with negligible latency overhead.

## E Evaluation metrics

We provide formal definitions of all evaluation metrics used in the three benchmarks.

### BiasBios.

- **Top-1 Accuracy.** The generated text is parsed for an occupation label. If the predicted occupation matches the ground-truth target, the sample is correct. Accuracy is the fraction of correct predictions over the test set.
- **Fluency.** Defined as the mean token-level log-probability of the generated text:

$$\text{Fluency} = \frac{1}{T} \sum_{t=1}^T \log p(x_t | x_{<t}) \quad (11)$$

where  $T$  is the number of generated tokens. Higher values indicate more fluent, confident generation.

- **Consistency.** The cosine similarity between the mean hidden state of the generated text and the mean hidden state of the input context, averaged over all samples. This measures whether the generation stays semantically aligned with the input.

**CounterFact.**

- **Efficacy Score.** The probability that the model assigns higher likelihood to the target answer than to the original (pre-edit) answer:

$$\text{Efficacy} = \frac{1}{|\mathcal{D}|} \sum_{(s, o^*, o) \in \mathcal{D}} \mathbf{1}[p(o^* | s) > p(o | s)] \quad (12)$$

where  $s$  is the subject prompt,  $o^*$  is the target (counterfactual) object, and  $o$  is the original object.

- **Paraphrase Score.** Same as Efficacy, but evaluated on paraphrased versions of the subject prompt, measuring robustness to surface-form variation.

**Pronoun Change.** Given an input biography containing gendered pronouns and an instruction to replace them with gender-neutral forms, two metrics are computed based on the generated text:

- **P. Score** (basic pronoun conversion rate). Let  $\mathcal{P}_b = \{\text{she, he}\}$  be the basic pronoun set. For each sample, count the number of basic pronouns in the original text ( $n_b$ ) and the number still remaining in the generated text ( $r_b$ ). The conversion rate is  $(n_b - r_b)/n_b$ . This is multiplied by the content overlap ratio (fraction of non-pronoun content tokens preserved) to penalize generations that trivially remove pronouns by truncating the text:

$$\text{P. Score} = \frac{n_b - r_b}{n_b} \times \frac{|\text{content}_{\text{gen}} \cap \text{content}_{\text{orig}}|}{|\text{content}_{\text{orig}}|} \quad (13)$$

- **All-changed P. Score.** Same formula but with the extended pronoun set  $\mathcal{P}_a = \{\text{she, he, her, him, hers, his, herself, himself}\}$ . Because  $\mathcal{P}_b \subset \mathcal{P}_a$  but the denominators differ ( $n_b$  vs.  $n_a$ ), it is mathematically possible for All-changed to exceed P. Score when the model converts extended forms more successfully than basic ones.

## F Comparison with AdaSEKA

AdaSEKA [Li et al., 2026] extends SEKA with a query-adaptive multi-expert routing mechanism that dynamically selects among multiple projection subspaces based on the input query’s semantic intent. While this achieves strong performance on several benchmarks, it comes at substantial computational cost: +0.27 s latency ( $9\times$  PRISM- $\Delta$ ) and +15.59 GB peak memory, placing it in a fundamentally different efficiency regime from single-projection methods like SEKA and PRISM- $\Delta$ .

Table 8 provides the full comparison. Key observations:

- **On BiasBios**, the best lightweight method outperforms AdaSEKA on 4 out of 5 models. PRISM- $\Delta$  leads on all three Qwen3 models, while SEKA leads on GEMMA3-12B with the largest margin of +1.90%. AdaSEKA wins only on GEMMA3-4B by 0.02%.
- **On CounterFact**, PRISM- $\Delta$  surpasses SEKA on 4 of 5 models and matches it on the fifth (GEMMA3-12B: both 98.86%). All methods operate near the performance ceiling (98–99%), so absolute differences are small.
- **On Pronoun Change**, AdaSEKA achieves the highest scores on 3 out of 5 models (QWEN3-8B/14B, GEMMA3-4B). However, on QWEN3-4B and GEMMA3-12B, the best lightweight method surpasses AdaSEKA.
- **Overall**, among the 15 model  $\times$  benchmark cells, the best lightweight method matches or exceeds AdaSEKA in **10 out of 15 cases**, despite using  $9\times$  less latency and negligible additional memory.

The multi-expert routing of AdaSEKA helps most on Pronoun Change with GEMMA3-4B, but does not justify its overhead in the majority of settings. PRISM- $\Delta$  matches or exceeds AdaSEKA on 10 of 15 cells at a fraction of the cost.

Table 8: Full comparison including AdaSEKA (%). **Bold**: best among lightweight methods; underline: best overall (including AdaSEKA).

|             | Model      | SEKA         | PRISM- $\Delta$ | PRISM- $\Delta V$ | AdaSEKA      | $\Delta$ (best lightweight – AdaSEKA) |
|-------------|------------|--------------|-----------------|-------------------|--------------|---------------------------------------|
| BiasBios    | QWEN3-4B   | 90.92        | <b>92.38</b>    | 92.36             | 91.86        | +0.52                                 |
|             | QWEN3-8B   | 88.74        | <b>89.62</b>    | 89.12             | 88.50        | +1.12                                 |
|             | QWEN3-14B  | 90.28        | <b>91.68</b>    | 91.20             | 91.22        | +0.46                                 |
|             | GEMMA3-4B  | 92.42        | <b>92.90</b>    | 91.64             | <u>92.92</u> | -0.02                                 |
|             | GEMMA3-12B | <b>93.04</b> | 92.22           | 91.94             | 91.14        | +1.90                                 |
| CounterFact | QWEN3-4B   | 99.02        | <b>99.14</b>    | 98.08             | 98.90        | +0.24                                 |
|             | QWEN3-8B   | 99.08        | <b>99.24</b>    | 98.46             | 99.00        | +0.24                                 |
|             | QWEN3-14B  | 98.92        | <b>99.00</b>    | 98.98             | 99.00        | 0.00                                  |
|             | GEMMA3-4B  | 98.04        | <b>98.10</b>    | 97.68             | <u>98.74</u> | -0.64                                 |
|             | GEMMA3-12B | <b>98.86</b> | <b>98.86</b>    | 93.40             | 92.48        | +6.38                                 |
| Pronoun     | QWEN3-4B   | 95.18        | <b>96.18</b>    | 96.06             | 94.54        | +1.64                                 |
|             | QWEN3-8B   | 98.56        | 99.40           | <b>99.48</b>      | 99.68        | -0.20                                 |
|             | QWEN3-14B  | 98.66        | <b>99.66</b>    | <b>99.66</b>      | <u>99.88</u> | -0.22                                 |
|             | GEMMA3-4B  | 81.53        | 89.08           | <b>90.16</b>      | <u>93.76</u> | -3.60                                 |
|             | GEMMA3-12B | 97.70        | <b>97.94</b>    | 94.54             | 96.88        | +1.06                                 |

## G Hyperparameters

Tables 9 and 10 list the optimal hyperparameters for PRISM- $\Delta$  and PRISM- $\Delta V$  respectively. Hyperparameters are tuned via grid search on the validation set.

The gain  $g_K$  varies across benchmarks:  $\sim 0.40$  for BiasBios, 1.10–6.00 for CounterFact, and 0.05–0.30 for Pronoun Change, reflecting different steering intensities per task. The variance retention threshold  $\gamma$  is high for Qwen3 but lower for Gemma3. On GEMMA3-12B (Pronoun Change),  $g_K = -0.30$ ; see Section 7 for discussion.

Table 9: PRISM- $\Delta$  hyperparameters.

| Model      | Benchmark      | $\gamma$ | $\delta_{\min}$ | $g_K$ |
|------------|----------------|----------|-----------------|-------|
| QWEN3-4B   | BiasBios       | 0.998    | 0.08            | 0.40  |
| QWEN3-8B   |                | 0.998    | 0.08            | 0.40  |
| QWEN3-14B  |                | 0.998    | 0.08            | 0.40  |
| GEMMA3-4B  |                | 0.850    | 0.08            | 0.50  |
| GEMMA3-12B |                | 0.980    | 0.00            | 0.40  |
| QWEN3-4B   | CounterFact    | 0.998    | 0.13            | 1.90  |
| QWEN3-8B   |                | 0.960    | 0.12            | 2.70  |
| QWEN3-14B  |                | 0.870    | 0.08            | 3.00  |
| GEMMA3-4B  |                | 0.990    | 0.12            | 6.00  |
| GEMMA3-12B |                | 0.990    | 0.50            | 1.10  |
| QWEN3-4B   | Pronoun Change | 0.880    | 0.15            | 0.15  |
| QWEN3-8B   |                | 0.900    | 0.15            | 0.05  |
| QWEN3-14B  |                | 0.880    | 0.15            | 0.05  |
| GEMMA3-4B  |                | 0.800    | 0.15            | 0.30  |
| GEMMA3-12B |                | 0.700    | 0.30            | -0.30 |

## H Detailed experimental setup

**Hardware.** All experiments are conducted on NVIDIA H20 GPUs with 144 GB memory. Projection construction uses a single GPU; evaluation uses a single GPU with batch size 256 for BiasBios and CounterFact, and batch size 1 for Pronoun Change.

**Data splits.** For BiasBios, we evaluate on the first 5000 samples (indices 0–4999); a 500-sample validation subset is used for hyperparameter tuning. For CounterFact, samples 0–5000 serve as the

Table 10: PRISM- $\Delta V$  hyperparameters.

| Model      | Benchmark      | $\gamma$ | $\delta_{\min}$ | $g_K$ | $g_V$ |
|------------|----------------|----------|-----------------|-------|-------|
| QWEN3-4B   | BiasBios       | 0.998    | 0.08            | 0.40  | 0.10  |
| QWEN3-8B   |                | 0.998    | 0.08            | 0.40  | 0.10  |
| QWEN3-14B  |                | 0.998    | 0.08            | 0.40  | 0.10  |
| GEMMA3-4B  |                | 0.800    | 0.12            | 0.30  | 0.10  |
| GEMMA3-12B |                | 0.994    | 0.00            | 0.40  | 0.10  |
| QWEN3-4B   | CounterFact    | 0.998    | 0.13            | 1.90  | 0.02  |
| QWEN3-8B   |                | 0.960    | 0.12            | 2.70  | 0.05  |
| QWEN3-14B  |                | 0.870    | 0.08            | 3.00  | 0.05  |
| GEMMA3-4B  |                | 0.990    | 0.12            | 6.00  | 0.10  |
| GEMMA3-12B |                | 0.990    | 0.40            | 3.00  | 0.50  |
| QWEN3-4B   | Pronoun Change | 0.880    | 0.15            | 0.15  | 0.05  |
| QWEN3-8B   |                | 0.900    | 0.15            | 0.05  | 0.02  |
| QWEN3-14B  |                | 0.880    | 0.15            | 0.05  | 0.02  |
| GEMMA3-4B  |                | 0.800    | 0.15            | 0.30  | 0.10  |
| GEMMA3-12B |                | 0.700    | 0.30            | 0.05  | 0.02  |

validation set and samples 5000–10000 as the test set. Pronoun Change uses 500 validation and 500 test samples following Li et al. [2026].

**Evaluation protocol.** All methods use greedy decoding with a maximum of 64 new tokens for BiasBios, 32 for CounterFact, and 128 for Pronoun Change. We report Top-1 Accuracy for BiasBios, Efficacy and Paraphrase scores for CounterFact, and P. Score and All-changed P. Score for Pronoun Change. Fluency is measured as the mean log-probability of generated tokens, and Consistency as the cosine similarity between the generation embedding and the context embedding.

**Contrastive data.** The 100 synthetic contrastive QA pairs are generated by GPT-4o. Each pair contains two unrelated text contexts paired with two questions, one relevant and one irrelevant to each context. This yields 200 contrastive triplets from which Key and Value representations are extracted at the answer token position.

**Projection construction.** For each model, we extract representations from all layers and heads under three prompting conditions (neutral, positive, negative). The differential cross-covariance  $\Omega_{\Delta}$  is computed per head, followed by SVD. The top- $k$  singular vectors are retained based on the cumulative energy threshold  $\gamma$ . The norm of the retained singular values determines the head’s discriminability score  $D_{\ell,h}$ , which is mapped to a weight via softplus. The entire process takes 3–8 minutes per model depending on model size.

**Lost-in-the-Middle setup.** We use the NaturalQuestions-based benchmark of Liu et al. [2024] with 30 passages per input, where one gold passage contains the answer and the remaining 29 are distractors. The gold passage is placed at 7 positions (0, 4, 9, 14, 19, 24, 29) to probe positional sensitivity. Steering is applied selectively to the middle region (passages 4–25), targeting the positional recall deficit. Generation is limited to 60 tokens. We report Exact Match averaged across all 7 positions.

## I Cross-model K/V complementarity

Table 11 and Figure 7 show that both Key and Value channels carry discriminative signal across all five models, but the balance between them differs substantially.

**Qwen3 family.** Value signal grows with model size (K/V ratio: 1.02  $\rightarrow$  0.74  $\rightarrow$  0.58). On QWEN3-14B, Value signal is nearly twice as strong as Key, and Figure 7 shows clear Value dominance in late

Table 11: Key and Value discriminative signal strength across models (BiasBios, mean norm\_diff over all heads).

| Model      | Layers | Heads | K mean | V mean | K/V ratio |
|------------|--------|-------|--------|--------|-----------|
| QWEN3-4B   | 36     | 8     | 0.137  | 0.135  | 1.02      |
| QWEN3-8B   | 36     | 8     | 0.129  | 0.174  | 0.74      |
| QWEN3-14B  | 40     | 8     | 0.138  | 0.237  | 0.58      |
| GEMMA3-4B  | 34     | 4     | 0.451  | 0.338  | 1.33      |
| GEMMA3-12B | 48     | 8     | 0.509  | 0.420  | 1.21      |

layers (L30+). The Value channel’s primary benefit is generation quality preservation (Table 5) rather than accuracy, consistent with its role as the content channel.

**Gemma3 family.** Both models exhibit 3–4× higher absolute norm\_diffs than Qwen3 (K mean: 0.45–0.51 vs. 0.13–0.14), indicating much stronger differential signal. Key dominates throughout all layers (K/V ratio > 1.2). This elevated signal magnitude explains why Gemma3 models require smaller gain values ( $g_K \approx 0.30$ – $0.40$ ) to avoid over-steering.

The observed correlation between norm\_diff magnitude and optimal gain (smaller  $g_K$  for Gemma3’s stronger signal) points toward a simple heuristic: scale  $g_K$  inversely with mean norm\_diff. The empirically optimal settings in Table 9 are consistent with this rule of thumb.

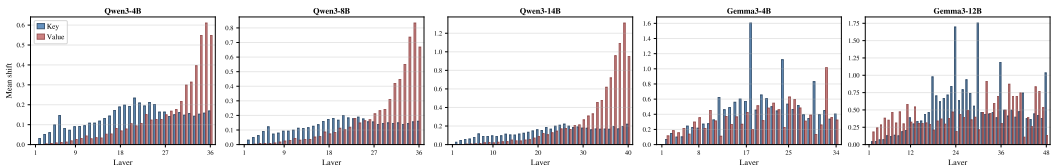


Figure 7: Layer-wise Key and Value discriminative signal across all five models. The depth profile varies by architecture: Qwen3 models show increasing Value dominance in late layers, while Gemma3 models maintain Key dominance throughout.

## J Projection stability across random seeds

To verify that results are stable across different training data, we construct five independent projections using different random seeds (1–5) with `max_samples=70`, so each seed selects a different subset of 70 from 100 available QA pairs (~70% overlap between subsets). All other hyperparameters are fixed ( $\gamma=0.998$ ,  $\delta_{\min}=0.08$ ,  $g_K=0.40$ ).

Table 12: Projection stability across independent data subsets (BiasBios, Top-1 Accuracy %).

| Seed              | QWEN3-4B            | QWEN3-8B            |
|-------------------|---------------------|---------------------|
| 1                 | 92.22               | 89.08               |
| 2                 | 92.12               | 89.34               |
| 3                 | 92.08               | 88.98               |
| 4                 | 92.14               | 89.30               |
| 5                 | 92.12               | 89.34               |
| <b>Mean ± Std</b> | <b>92.14 ± 0.05</b> | <b>89.21 ± 0.15</b> |

Table 12 shows that the standard deviation across five independent data subsets is very small: 0.05% on QWEN3-4B and 0.15% on QWEN3-8B. Both are far smaller than PRISM- $\Delta$ ’s improvement over SEKA, which is +1.46% on QWEN3-4B and +0.88% on QWEN3-8B. Combined with greedy decoding, which eliminates sampling variance at inference, the reported results are highly stable. The slightly higher variance on QWEN3-8B may reflect the larger model’s greater sensitivity to which specific contrastive examples are included, though both values remain negligible relative to the method’s gains.

## K Statistical reliability details

All results use greedy decoding, so inference is fully deterministic given a fixed projection. The only source of variance is projection construction. As shown in Appendix J, across five independent data subsets (70/100 samples each, i.e., 30% held out), the standard deviation is 0.05% on QWEN3-4B and 0.15% on QWEN3-8B—a conservative upper bound far smaller than the reported improvements.

Beyond individual margins, the *consistency* of gains across models provides strong evidence. PRISM- $\Delta$  matches or exceeds SEKA on 14 out of 15 model  $\times$  benchmark cells (one-sided sign test:  $p < 0.001$ ). Additionally, PRISM- $\Delta$  achieves strictly higher scores than SEKA on all five models for Pronoun Change P. Score ( $p = 0.031$ ) and on 4 out of 5 for CounterFact Efficacy (1 tied). Such cross-model consistency is unlikely to arise from noise.

## L Value gain sensitivity

Table 13: Value gain ( $g_V$ ) sensitivity on CounterFact (validation set, Efficacy %).  $g_K$  is fixed at each model’s optimal PRISM- $\Delta$  value.

| Model      | $g_K$ | $g_V=0.02$   | $g_V=0.05$   | $g_V=0.10$   | $g_V=0.30$ | $g_V=0.50$ | PRISM- $\Delta$ |
|------------|-------|--------------|--------------|--------------|------------|------------|-----------------|
| QWEN3-4B   | 1.90  | <b>98.38</b> | 98.32        | 98.20        | 97.52      | 96.48      | 99.14           |
| QWEN3-8B   | 2.70  | —            | <b>98.46</b> | 98.48        | 98.40      | —          | 99.24           |
| QWEN3-14B  | 3.00  | —            | <b>98.98</b> | 98.94        | —          | —          | 99.00           |
| GEMMA3-4B  | 6.00  | —            | —            | <b>98.06</b> | 97.76      | —          | 98.10           |
| GEMMA3-12B | 1.10  | —            | 62.42        | 62.88        | —          | —          | 98.86           |

Table 13 and Figure 8 report PRISM- $\Delta$ V performance as a function of the Value gain  $g_V$  on CounterFact. Across all models, smaller  $g_V$  values outperform larger ones, with the optimal range between 0.02 and 0.10. The discriminative signal for CounterFact is concentrated in the attention routing channel (Key), consistent with the cross-model analysis in Appendix I. Value steering is most beneficial for generation quality preservation (Table 5) rather than accuracy on knowledge conflict tasks.

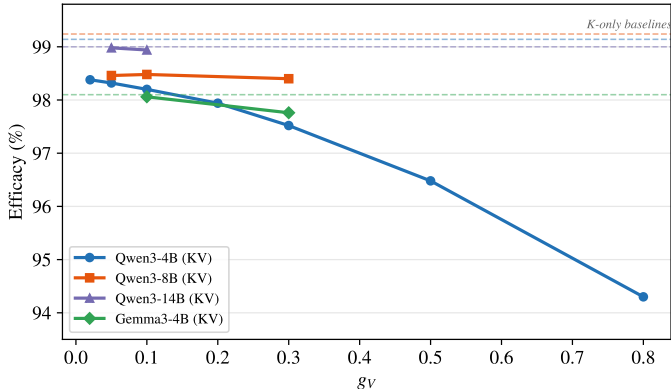


Figure 8: Value gain ( $g_V$ ) sensitivity on CounterFact. Solid lines: PRISM- $\Delta$ V Efficacy at varying  $g_V$ . Dashed lines: corresponding PRISM- $\Delta$  ( $g_V=0$ ) baselines. Smaller  $g_V$  is consistently better, but KV never surpasses K-only.

## M CounterFact ablation

Differential projection contributes +0.30%, computed as the gap between PRISM- $\Delta$  at 99.14% and the independent-projection variant at 98.84%. Softplus weighting contributes +0.52%, measured as the gap between PRISM- $\Delta$  and the uniform-weight variant at 98.62%. These are qualitatively consistent with the BiasBios ablation in Table 2.

Table 14: Ablation on CounterFact (QWEN3-4B, Efficacy %, test set). Higher gain ( $g_K=1.90$ ) amplifies the contribution of each component compared to BiasBios ( $g_K=0.40$ ).

| Configuration     | Projection   | Weighting | Efficacy (%) |
|-------------------|--------------|-----------|--------------|
| PRISM- $\Delta$   | Differential | Softplus  | <b>99.14</b> |
| Indep. + softplus | Independent  | Softplus  | 98.84        |
| Diff. + uniform   | Differential | Uniform   | 98.62        |

The smaller absolute contributions on CounterFact reflect the near-saturation regime, where all methods already operate between 98% and 99% Efficacy. In this regime, the headroom for improvement is inherently limited. Nonetheless, the relative ordering is preserved: softplus remains the larger contributor, and both components provide positive gains. This confirms that the coupling between differential projection and softplus weighting, first observed on BiasBios, generalizes to a different task type with much higher gain values.

## N Data quantity ablation

Table 15: Effect of synthetic data quantity on PRISM- $\Delta$  (BiasBios, QWEN3-4B).

| Synthetic samples | Top-1 Accuracy (%) |
|-------------------|--------------------|
| 50                | 91.92              |
| 100 (default)     | 92.38              |
| 200               | 92.40              |

Table 15 confirms that 50 samples already achieve 91.92% (only 0.46% below the default), and doubling from 100 to 200 yields negligible improvement (+0.02%), demonstrating high data efficiency. This rapid saturation is expected: the cross-covariance matrix  $\Omega_\Delta$  is a sum over samples, and its top singular directions stabilize quickly once sufficient contrastive signal is accumulated. In practice, 100 samples provide a good balance between projection quality and data collection cost.

## O Projection rank analysis

The rank  $k$  of each head’s projection matrix  $P_K = U_{:,k}U_{:,k}^\top$  is determined by the cumulative energy threshold  $\gamma$ : we retain the minimum number of singular vectors such that  $\sum_{i=1}^k \sigma_i^2 / \sum_{i=1}^d \sigma_i^2 \geq \gamma$ . Heads whose discriminability  $D_{\ell,h}$  falls below  $\delta_{\min}$  receive a zero-rank projection, effectively deactivating them.

Table 16: Projection rank statistics across models (BiasBios, Key channel). Active heads are those with  $D_{\ell,h} \geq \delta_{\min}$ .

| Model      | $d$ | Total | Active    | Rank min | Rank max | Rank mean | Rank median |
|------------|-----|-------|-----------|----------|----------|-----------|-------------|
| QWEN3-4B   | 128 | 288   | 242 (84%) | 70       | 110      | 95.6      | 96          |
| GEMMA3-4B  | 256 | 136   | 127 (93%) | 98       | 218      | 177.7     | 183         |
| GEMMA3-12B | 256 | 384   | 346 (90%) | 71       | 223      | 177.9     | 182         |

Table 16 reveals several patterns. First, the fraction of active heads ranges from 84% to 93%, meaning a substantial majority of heads carry discriminative signal above  $\delta_{\min}$ . Second, the retained rank is high relative to the head dimension: on QWEN3-4B, the median rank is 96 out of 128 dimensions, meaning the projection retains roughly 75% of the subspace. On Gemma3 models with  $d=256$ , the median rank of 182–183 retains about 71%.

This high rank reflects the  $\gamma=0.998$  variance threshold for Qwen3 and  $\gamma=0.85$ – $0.98$  for Gemma3: the differential cross-covariance has relatively spread singular spectra, so many components are needed to capture 99.8% of the energy. The projections are therefore not aggressive low-rank

approximations but rather gentle subspace restrictions that remove only the least discriminative 25–29% of dimensions.

## P Direction consistency

Table 17: Cross-head cosine similarity of top singular vectors (QWEN3-4B, 288 heads).

|                                      | $\Omega^+$ (independent) | $\Omega_\Delta$ (differential) | Random baseline |
|--------------------------------------|--------------------------|--------------------------------|-----------------|
| Cross-head similarity (mean)         | 0.254                    | <b>0.068</b>                   | 0.079           |
| Cross-head similarity (early layers) | 0.353                    | <b>0.053</b>                   | 0.079           |

To quantify whether different heads learn independent or redundant directions, we compute the mean pairwise absolute cosine similarity between the top left singular vectors of all 288 heads (QWEN3-4B, 36 layers  $\times$  8 heads). A random baseline is computed by averaging cosine similarities between uniformly sampled unit vectors in  $\mathbb{R}^{128}$ , yielding 0.079.

As shown in Table 17,  $\Omega^+$  directions exhibit high cross-head similarity (0.254), over  $3\times$  the random baseline. This confirms that independent SVD on  $\Omega^+$  is dominated by shared structural directions common to many heads—precisely the redundancy that Proposition 1(b) predicts differential decomposition will remove. In contrast,  $\Omega_\Delta$  directions achieve 0.068, slightly *below* the random baseline, indicating that each head extracts a nearly independent discriminative direction. The sub-random value likely reflects a mild orthogonality bias: since all heads optimize over the same finite input data, SVD solutions tend to avoid directions already captured by other heads.

The effect is even more pronounced in early layers (L1–12), where  $\Omega^+$  similarity rises to 0.353 while  $\Omega_\Delta$  drops to 0.053. Early layers encode more generic, shared features, so the benefit of differential projection—filtering out these shared directions—is strongest there.

## Q Hyperparameter sensitivity

We sweep each hyperparameter independently while holding others at their optimal values (QWEN3-4B, BiasBios).

**$g_K$  sensitivity.** The optimal region is  $g_K \in [0.35, 0.50]$ , within which performance varies by less than 0.5%. Performance degrades gracefully outside this range.

**$\delta_{\min}$  sensitivity.** The optimal region is  $\delta_{\min} \in [0.06, 0.10]$ , with performance variation less than 0.4%.

**$\gamma$  sensitivity.** Performance is nearly invariant to  $\gamma$  in  $[0.990, 0.998]$  (variation  $< 0.1\%$ ), indicating that PRISM- $\Delta$  is robust to the choice of variance retention threshold.

**Cross-model  $g_K$ .** Figure 9 indicates that the optimal  $g_K$  is  $\sim 0.40$  for both Qwen3 and GEMMA3-12B, and  $\sim 0.30$  for GEMMA3-4B, showing reasonable cross-architecture consistency.

## R Case study

We identify 154 samples (33.9% of SEKA’s 454 errors on BiasBios with QWEN3-4B) where SEKA predicts incorrectly but PRISM- $\Delta$  succeeds. Figure 6b reveals that PRISM- $\Delta$  rescues 154 samples while losing only 81, for a net gain of 73 samples (+1.46% accuracy). Representative examples:

**Success cases.** The following examples illustrate contexts where SEKA fails but PRISM- $\Delta$  succeeds:

- “*PhD, Adjunct Assistant Professor in Psychiatry...*”  $\rightarrow$  SEKA: psychologist; PRISM- $\Delta$ : **professor** ✓
- “*assistant professor of psychology at NUS...*”  $\rightarrow$  SEKA: psychologist; PRISM- $\Delta$ : **professor** ✓

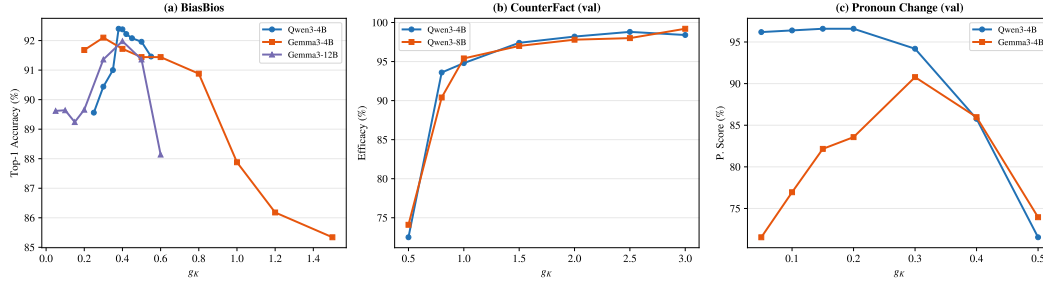


Figure 9: Gain sweep curves across three benchmarks, showing performance as a function of  $g_K$  for different models. The optimal region is broad ( $g_K \in [0.35, 0.50]$  for BiasBios), indicating low sensitivity.

- “Performance Architect at Cisco...” → SEKA: software engineer; PRISM- $\Delta$ : **architect** ✓
- “aspiring filmmaker...shoots promotional videos...” → SEKA: photographer; PRISM- $\Delta$ : **filmmaker** ✓
- “is a Maine comedian...” → SEKA: photographer; PRISM- $\Delta$ : **comedian** ✓

In most rescued cases, the occupation keyword co-occurs with a semantically related domain word or company name that sways SEKA’s projection. For instance, “Psychiatry” and “psychology” pull SEKA toward “psychologist” even when the biography clearly describes a professor. Similarly, “Cisco” triggers a “software engineer” prediction despite “Architect” appearing explicitly. PRISM- $\Delta$ ’s differential projection suppresses these shared domain features and more precisely isolates the occupation-describing signal, consistent with the shared-direction elimination guaranteed by Proposition 1(b).

**Failure analysis.** Among the 81 samples where PRISM- $\Delta$  gets wrong but SEKA succeeds, the biographies tend to contain very short or ambiguous occupation descriptions where the differential signal is inherently weak. The 2:1 ratio (154 rescued vs. 81 lost) confirms that PRISM’s net effect is strongly positive.